Novel magnetic resonance technique for functional imaging of cystic fibrosis lung disease

Sylvia Nyilas[1,9], Grzegorz Bauman[2,3,9], Gregor Sommer[4], Enno Stranzinger[5,6], Orso Pusterla[2,3], Urs Frey[7], Insa Korten[1], Florian Singer[1,8], Carmen Casaulta[1], Oliver Bieri[2,3,10] and Philipp Latzin[1,10]

Affiliations: [1]Pediatric Respiratory Medicine, Dept of Pediatrics, Inselspital, Bern University Hospital, University of Bern, Bern, Switzerland. [2]Dept of Radiology, Division of Radiological Physics, University of Basel Hospital, Basel, Switzerland. [3]Dept of Biomedical Engineering, University of Basel, Basel, Switzerland. [4]Clinic of Radiology and Nuclear Medicine, University of Basel Hospital, Basel, Switzerland. [5]Dept of Interventional and Pediatric Radiology, Inselspital, Bern University Hospital, Bern, Switzerland. [6]Division of Radiological Physics, Clinic of Radiology and Nuclear Medicine, University of Bern Hospital, Bern, Switzerland. [7]University Children's Hospital Basel (UKBB), Basel, Switzerland. [8]Division of Respiratory Medicine, University Children's Hospital Zurich, Zurich, Switzerland. [9]Contributed equally as first authors. [10]Contributed equally as senior authors.

Correspondence: Philipp Latzin, University Children's Hospital of Bern, Freiburgstrasse 8, 3010 Bern, Switzerland. E-mail: philipp.latzin@insel.ch

@ERSpublications
New functional MRI without the need for contrast agents correlates strongly with ventilation inhomogeneity in CF http://ow.ly/emo930eQJ67

Cite this article as: Nyilas S, Bauman G, Sommer G, *et al*. Novel magnetic resonance technique for functional imaging of cystic fibrosis lung disease. *Eur Respir J* 2017; 50: 1701464 [https://doi.org/10.1183/13993003.01464-2017].

ABSTRACT Lung function tests are commonly used to monitor lung disease in cystic fibrosis (CF). While practical, they cannot locate the exact origin of functional impairment. Contemporary magnetic resonance imaging (MRI) techniques provide information on the location of disease but the need for contrast agents constrains their repeated application. We examined the correlation between functional MRI, performed without administration of contrast agent, and lung clearance index (LCI) from nitrogen multiple-breath washout (N_2-MBW).

40 children with CF (median (range) age 12.0 (6–18) years) and 12 healthy age-matched controls underwent functional and structural MRI and lung function tests on the same day. Functional MRI provided semiquantitative measures of perfusion (R_Q) and ventilation (R_{FV}) impairment as percentages of affected lung volume. Morphological MRI was evaluated using CF-specific scores. LCI measured global ventilation inhomogeneity.

MRI detected functional impairment in CF: R_{FV} 19–38% and R_Q 16–35%. R_{FV} and R_Q correlated strongly with LCI (r=0.76, p<0.0001 and r=0.85, p<0.0001, respectively), as did total morphology score (r=0.81, p<0.0001). All indices differed significantly between patients with CF and healthy controls (p<0.001).

Noninvasive functional MRI is a promising method to detect and visualise perfusion and ventilation impairment in CF without the need for contrast agents.

This article has supplementary material available from erj.ersjournals.com

Received: Jan 13 2017 | Accepted after revision: Aug 31 2017

Support statement: The work for this report was funded by the Swiss National Foundation (grant SNF 320030_149576), Swiss Cystic Fibrosis Foundation (CFCH) and Botnar Foundation. The funders had no role in study design, data collection and analysis, decision to publish or preparation of the manuscript. Funding information for this article has been deposited with the Crossref Funder Registry.

Conflict of interest: Disclosures can be found alongside this article at erj.ersjournals.com

Introduction

Chronic lung diseases are highly prevalent in both children and adults. One of the most severe chronic lung diseases in childhood is cystic fibrosis (CF). CF is the most common autosomal recessive genetic disease in Caucasians [1]. Early diagnosis by newborn screening and improvement of therapy has raised interest in diagnostic tools to detect lung function impairment early and prior to irreversible lung damage [2–4]. Current techniques such as nitrogen multiple-breath washout (N_2-MBW) or high-resolution computer tomography (HRCT) allow monitoring of early lung disease [5, 6]. However, both techniques are constrained by methodological drawbacks. N_2-MBW estimates global ventilation inhomogeneity by the lung clearance index (LCI), but does not provide the exact location of underlying changes and more specific indices for ventilation inhomogeneities are not yet widely used [7, 8]. The cumulative radiation exposure of HRCT is low [9–11], but problematic for routine follow-up, and breathing manoeuvres are demanding for younger children.

In this regard, magnetic resonance imaging (MRI) is a rapidly evolving, radiation-free imaging technique to investigate the morphology and function of the lungs [12, 13]. Nonproton MRI techniques with inhaled hyperpolarised gaseous tracers such as ^{3}He and ^{129}Xe have been shown to provide the best static and dynamic ventilation image quality [14–16]. Nevertheless, the clinical application of these techniques is impeded by limited availability and the high costs of gases, hardware and trained personnel. Alternatively, pulmonary ventilation can also be assessed by proton MRI using T1-shortening oxygen as a gaseous tracer [17]. A recent study using promising contrast enhancement MRI [18, 19] showed a close correlation between lung function and MRI outcomes [20]. A drawback of this method is the need for a contrast agent and possible adverse effects, *e.g.* painful procedures, allergic reactions or neuronal tissue deposition of contrast media [21, 22].

To overcome those drawbacks, a new MRI technique, termed matrix pencil (MP) decomposition, a derivative of the Fourier decomposition (FD) method, was developed for evaluation of regional fractional ventilation and relative perfusion of the lung [23]. This novel MRI technique provides visual and numeric information of functional deficits in perfusion and ventilation domains of the lung. Importantly, intravenous contrast, inhaled tracers or breath-holding manoeuvres are not required; the technique is applicable during free tidal breathing.

The aim of this study was to assess whether indices from functional MRI differ between healthy controls and patients with CF. We further analysed the correlation between this new functional MRI method and N_2-MBW in children with CF. We hypothesised that functional MRI detects fractional ventilation and relative perfusion defects in CF lung disease and that these indices relate to lung function.

Methods

Study design

This was a prospective, cross-sectional, single-centre, observational study at the University Children's Hospital of Bern, Bern, Switzerland, conducted between February 2016 and May 2017. Participants underwent N_2-MBW, spirometry, body plethysmography and MRI on the same day, in that order.

Study population

We enrolled 40 unselected children with CF (supplementary table E1) across a wide age range (6–18 years), irrespective of bacterial colonisation or antibiotic use, to ensure a broad range of disease severity. Eligibility criteria were a confirmed diagnosis of CF, the ability to perform pulmonary function tests and MRI, and not requiring supplemental oxygen therapy. Healthy age-matched controls had neither a history of chronic lung disease nor acute respiratory infection in the 4 weeks prior to the investigations. The study was approved by the Ethics Committee of Bern (EKNZ 2015-326 and KEK 2017-00279). We obtained written informed consent from parents and participants, if older than 14 years.

MRI data acquisition and evaluation

Examinations were performed on a 1.5 T whole-body MRI scanner (MAGNETOM Aera; Siemens Healthineers, Erlangen, Germany) using a 12-channel thorax and a 24-channel spine receiver coil array. Sedation was not applied. Parents or caregivers were allowed to accompany children in the scanner cabin during imaging. Functional MRI scans were followed by morphological MRI scans. Regional fractional lung ventilation and relative perfusion were assessed using MP-MRI to acquire multiple coronal slices to cover the whole lung volume with a time-resolved ultra-fast steady-state free precession pulse sequence [24]. Details of scan parameters are given in supplementary table E2. Voxel distributions were used to estimate functional impairment. A similar thresholding method was used previously in a study comparing FD-MRI with dynamic contrast-enhanced MRI in CF patients [25]. For sensitivity analysis we additionally used 60% deviation as cut-off. The primary outcomes were percentage of the lung volume with impaired fractional

ventilation R_{FV} and relative perfusion R_Q (supplementary figure E1), and morphological assessment based on a protocol previously described by EICHINGER *et al.* [26] for MRI in CF (supplementary table E3). Secondary outcomes were diagnostic quality, measurement duration (supplementary material) and interobserver agreement between the two readers.

Lung function testing

N_2-MBW was performed with an unmodified device (Exhalyzer D; Eco Medics, Duernten, Switzerland) according to consensus [27]. Primary outcome was the LCI, calculated as cumulative expired volume over functional residual capacity, for global ventilation inhomogeneity. Secondary outcomes were phase III slope indices S_{cond} and S_{acin} for convection- and diffusion convection-dependent ventilation inhomogeneity, respectively [27].

Spirometry and body plethysmography (Jaeger MasterScreen; CareFusion, Hochberg, Germany) were performed after N_2-MBW, according to European Respiratory Society/American Thoracic Society guidelines [28]. Outcomes were forced expiratory volume in 1 s (FEV_1) and forced vital capacity from spirometry, and the ratio of residual volume and total lung capacity (RV/TLC).

Statistical analysis

We first assessed differences in MRI and lung function indices between patients with CF and healthy controls. In a second step we examined a possible correlation between functional indices from MRI and lung function. In a third step we examined the correlation between the morphological pathologies and lung function. For this, we used the mean of the morphological scores from both readers. Upper limit of normal was calculated using the mean+1.64SD of equipment-specific reference values for N_2-MBW [29] and data from healthy age-matched controls for functional MRI indices. Continuous variables were compared with the Wilcoxon–Mann–Whitney test, as appropriate. All correlations were described with Spearman's rank correlation coefficient (r). Interobserver agreement was calculated using the intraclass correlation coefficient (ICC). In general, ICC was defined as very good (>0.80), good (0.6–0.80) or moderate (0.4–0.59) [30]. p-values <0.05 were considered statistically significant. As appropriate, Bonferroni correction was used for multiple comparisons. Analyses were performed using Stata version 13 (StataCorp, College Station, TX, USA) and Matlab version 2012b (MathWorks, Natick, MA, USA). Additional details and the sample size calculation are provided in the supplementary material.

Results

Participants

MRI scans, N_2-MBW, spirometry and body plethysmography were successfully performed in all 40 patients with CF (median (range) age 12.0 (6–18) years) and all 12 healthy controls (median (range) age 12.0 (5–17) years). Characteristics of study participants are presented in supplementary table E1.

Data quality and measurement duration

Fractional ventilation and relative perfusion images were feasible and generated for all datasets obtained. In patients with CF, the mean (range) duration of the functional MRI scans was 5.6 (4.4–8.1) min and of the morphological MRI scans was 18.2 (13.2–24.6) min (supplementary table E4). Values were similar in healthy controls (supplementary table E5). Functional and morphological images from one healthy participant, one patient with a mild course of CF and one patient with a severe course of CF (based on FEV_1 values) are shown in figures 1, 2 and 3, respectively.

Comparison between healthy controls and patients with CF

Fractional ventilation impairment from functional MRI differed significantly between healthy controls and patients with CF (median (IQR) 17.1 (14.6–20.6) *versus* 29.4 (24.9–31.9); p<0.001) (supplementary figure E2). Likewise relative perfusion impairment differed significantly between both groups (median (IQR) 15.1 (13.4–17.4) *versus* 27.1 (22.9–29.2); p<0.001) (supplementary figure E3). Morphological MRI score revealed minimal structural changes in only four healthy controls (for both readers total score ranged from 0 to 3), while showing a wide range of structural changes in patients with CF (supplementary table E4). Indices from N_2-MBW differed significantly between groups, as to a lesser degree did some outcomes from spirometry and body plethysmography (supplementary table E6).

Interestingly, two patients with CF had results within the normal range in all functional modalities, two patients with CF showed compromised relative perfusion and fractional ventilation while LCI was within normal limits, and 17 patients with CF had normal FEV_1 results, but compromised fractional ventilation and relative perfusion assessed by functional MRI (figures 4a and b, and supplementary figures E4 and E5).

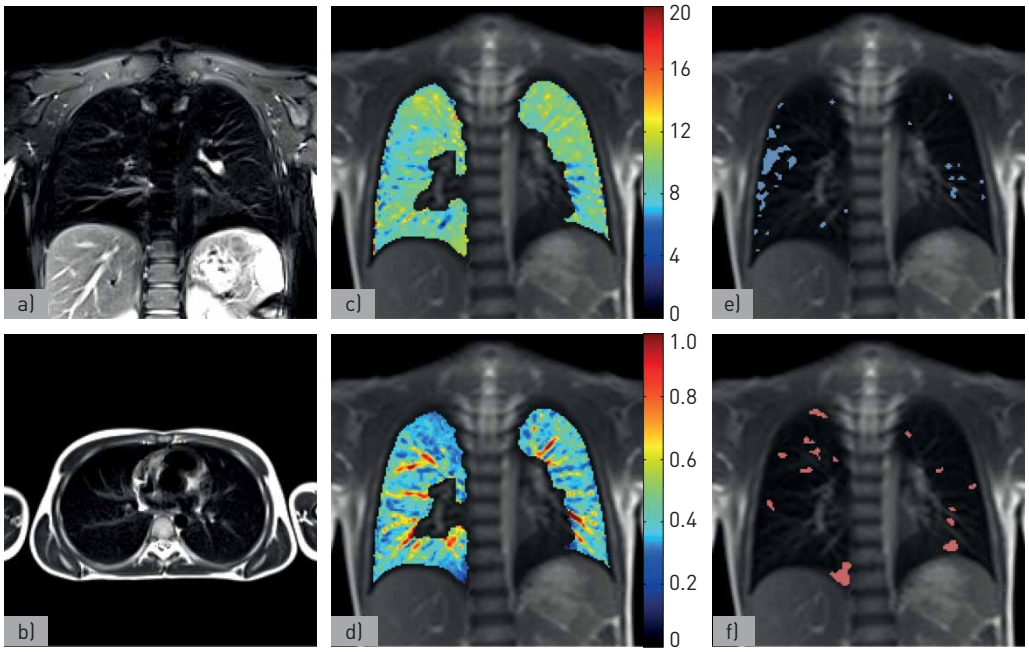

FIGURE 1 Example of a healthy child: a 7-year-old healthy boy. a) Coronal and b) axial 5-mm T2-weighted BLADE and HASTE (half-Fourier acquisition single-shot turbo spin-echo) images, respectively. Chest magnetic resonance imaging (MRI) was normal. c, d) Functional MRI shows fairly homogeneous distribution of c) fractional ventilation as well as d) relative perfusion. Small regions in both lungs were classified as hypoperfused as well as peripheral regions in the middle lobe of the right lung as hypoventilated. e, f) Masks overlaid on morphological images present e) fractional ventilation defects (5% of the slice area) and f) perfusion defects (4% of the slice area). Both lung clearance index (5.7 lung turnovers) and forced expiratory volume in 1 s (–0.30 z-scores) were normal.

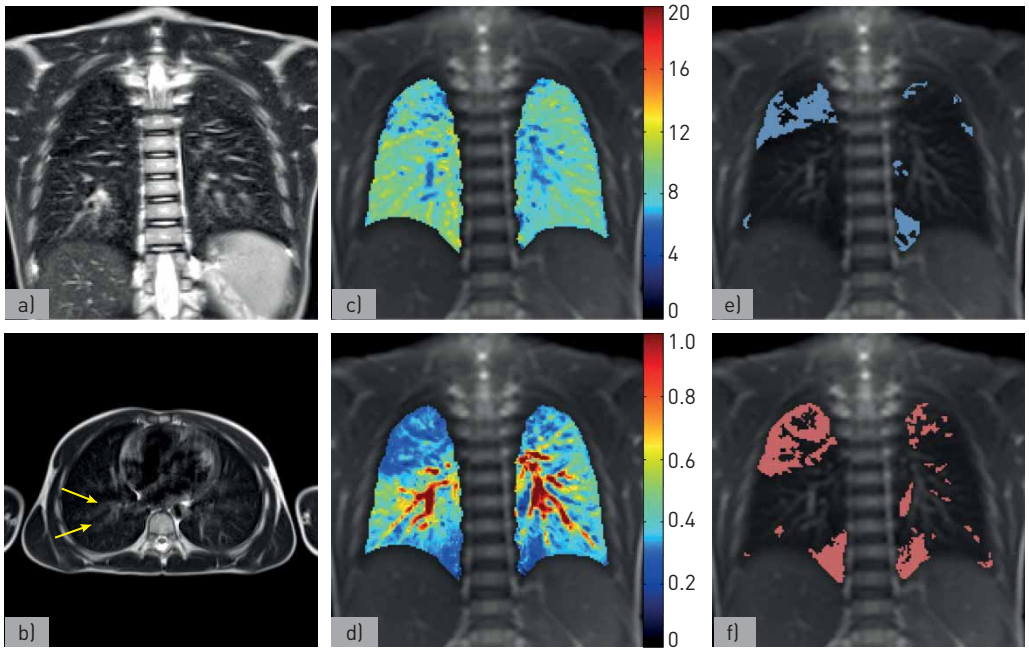

FIGURE 2 Example of a child with mild lung disease: a 9-year-old boy with cystic fibrosis. a) Coronal and b) axial 5-mm T2-weighted HASTE (half-Fourier acquisition single-shot turbo spin-echo) sequences. Mild bronchial wall thickening (b, arrows) is noted in the right lower lobe (Eichinger Score 1 (R1)). Otherwise normal chest magnetic resonance imaging (MRI). c) Functional MRI shows two main areas with reduced fractional ventilation located in the upper lobe of the right lung and basal part of the left lung. d) Relative perfusion map shows several regions with reduced perfusion in both lungs. e, f) Masks overlaid on morphological images present e) fractional ventilation defects (16% of the slice area) and f) perfusion defects (19% of the slice area). Lung clearance index was at the upper limit of normal (8.4 lung turnovers) and forced expiratory volume in 1 s was normal (0.46 z-scores).

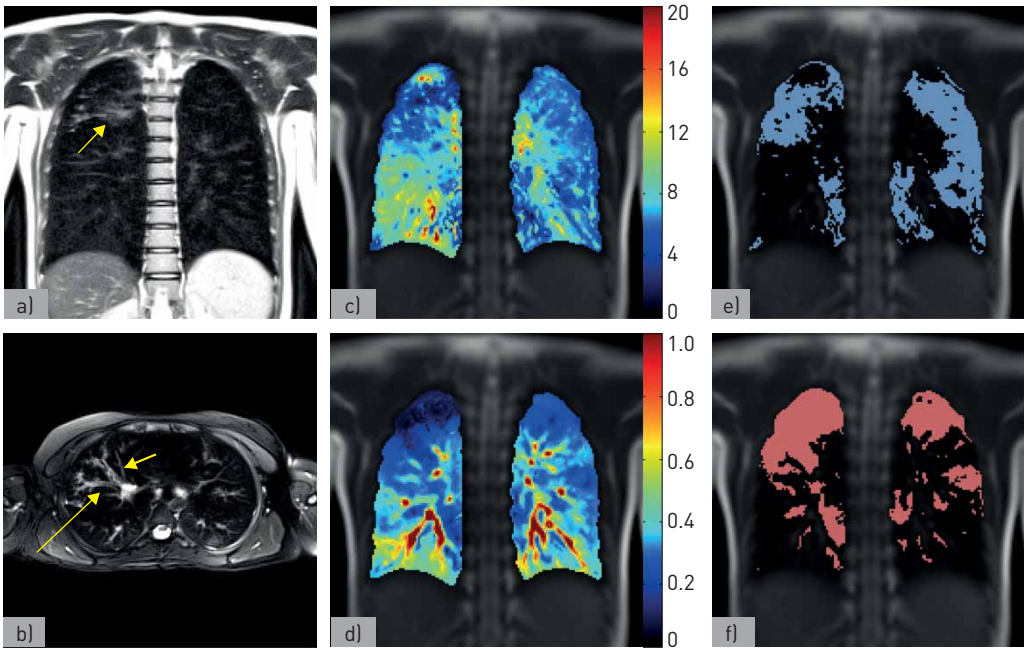

FIGURE 3 Example of a child with advanced lung disease: a 12-year-old girl with cystic fibrosis. a) Coronal HASTE (half-Fourier acquisition single-shot turbo spin-echo) sequence shows mild bronchiectasis and peribronchial infiltrates in the right upper lobe (arrow) (Eichinger Score 10 (R1)). b) Axial T2-weighted BLADE sequence shows moderate bronchial wall thickening in the right upper lobe (short arrow) and mucus plugging in the right upper lobe (long arrow). c, d) Functional magnetic resonance imaging shows c) large regions with reduced fractional ventilation, which are spatially matched with d) areas of decreased relative perfusion. e, f) Masks overlaid on morphological images present e) fractional ventilation defects (36% of the slice area) and f) relative perfusion defects (31% of the slice area). Both lung clearance index (13.4 lung turnovers) and forced expiratory volume in 1 s (−3.1 z-scores) showed pathological values.

Correlation between functional MRI and lung function in patients with CF

In patients with CF, the extent of impaired ventilation relative to lung volume (R_{FV}) quantified by functional MRI was between 19% and 38% (supplementary table E4). We found a strong correlation between R_{FV} and LCI (r=0.76, p<0.0001), as well as a correlation between R_{FV}, S_{cond} and S_{acin} (table 1 and figure 4a). We found a strong correlation between R_{FV} and FEV_1 (r=−0.64, p<0.0001) (supplementary figure E4). The RV/TLC ratio correlated with indices of functional MRI (table 1).

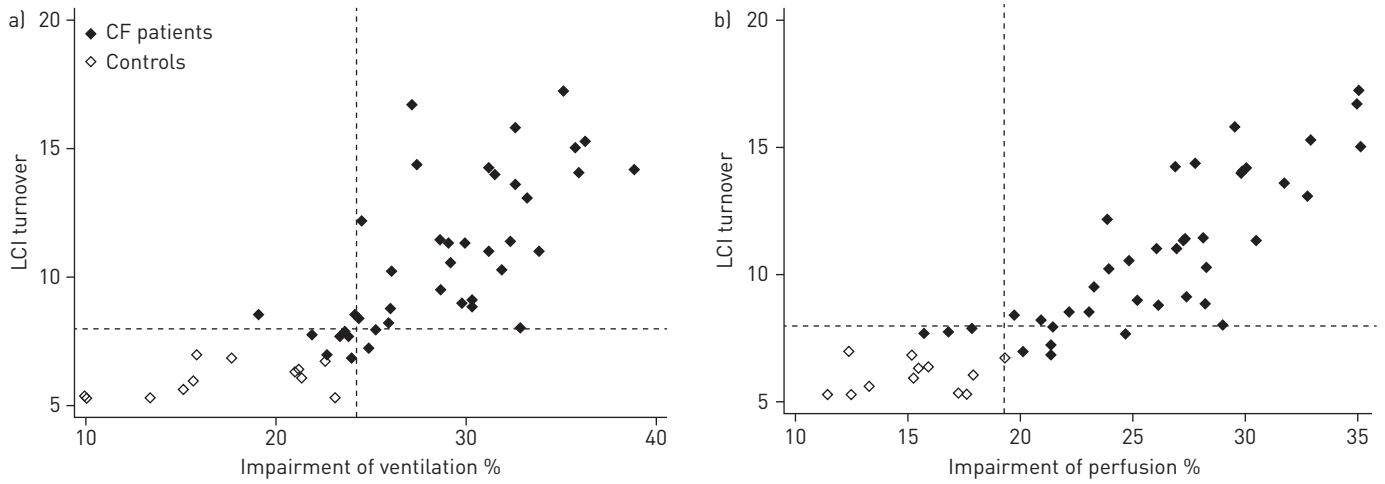

FIGURE 4 Correlation between lung clearance index (LCI) and impairment of the lung for patients with cystic fibrosis (CF) and healthy age-matched controls: a) fractional ventilation (R_{FV}) and b) relative perfusion (R_Q). Upper limit of normal is given as dashed lines for both modalities: LCI 8.0 lung turnovers, R_{FV} 24.2% and R_Q 19.3%.

TABLE 1 Functional magnetic resonance imaging (MRI) *versus* lung function outcomes in the 40 patients with cystic fibrosis

	R_{FV}		R_Q	
	r	p-value	r	p-value
LCI lung turnover	0.76	<0.0001#	0.85	<0.0001#
S_{cond} L^{-1}	0.55	0.0003#	0.62	<0.0001#
S_{acin} L^{-1}	0.49	0.0013#	0.44	0.0049
FEV_1 z-score	−0.64	<0.0001#	−0.67	<0.0001#
FVC z-score	−0.57	<0.0001#	−0.62	<0.0001#
RV/TLC %	0.54	0.0003#	0.59	0.0001#

Data are presented as Spearman correlation coefficients; for all correlations we performed a Bonferroni correction: 0.05/12, as appropriate. R_{FV}: impairment of ventilation; R_Q: impairment of perfusion; LCI: lung clearance index; S_{cond} and S_{acin}: normalised phase III slope indices (see main text and supplementary material for explanation); FEV_1: forced expiratory volume in 1 s; FVC: functional vital capacity; RV: residual volume; TLC: total lung capacity. Correlation between R_{FV} and R_Q from functional MRI (matrix pencil decomposition MRI) and different lung function outcomes: LCI, S_{cond}, S_{acin}, FEV_1, FVC and RV/TLC ratio. #: p-values <0.0042 were considered statistically significant.

The extent of impaired perfusion relative to lung volume (R_Q) was between 16% and 35% (supplementary table E4). R_Q showed a significant, excellent correlation with LCI (r=0.85, p<0.0001) (table 1 and figure 4b). S_{cond} also correlated with R_Q (r=0.62, p<0.0001) in comparison with a correlation between S_{acin} and R_Q (r=0.44, p=0.0049). We found a correlation between FEV_1 and R_Q (r=−0.67, p<0.0001) (supplementary figure E5). Changes in threshold by using 60% of the median value of the voxel distribution did not change the correlation between LCI, R_{FV} and R_Q (r=0.77, p<0.0001 and r=0.8, p<0.0001, respectively).

Correlation between morphological MRI score and lung function

The total morphology score in patients with CF ranged from 0 to 31 for both readers. For detailed subscores, see supplementary table E4. We found excellent correlation between LCI and total morphology scores (r=0.81, p<0.0001), as well as the subscores for bronchiectasis and bronchial wall thickening (r=0.81, p<0.0001) and mucus plugging (r=0.79, p<0.0001). We also found a correlation between the total morphology scores and S_{cond} (r=0.70, p<0.0001), as well as subscores. FEV_1 correlated with the total morphology score (r=−0.66, p<0.0001) (table 2).

Inter-reader correlation in patients with CF

Correlation between both readers was strong for total morphology score (r=0.84, p<0.0001), bronchiectasis/air wall thickening (r=0.73, p<0.0001) and mucus plugging (r=0.85, p<0.0001)

TABLE 2 Correlation between lung function parameters with magnetic resonance imaging (MRI)-defined morphological pathologies in lung structure in the 40 patients with cystic fibrosis

	Total score		Subscores									
	r	p-value	Wall thickening/ bronchiectasis		Mucus plugging		Consolidation		Abscess/ sacculation		Special findings	
			r	p-value	r	p-value	r	p-value	r	p-value	r	p-value
LCI lung turnover	0.81	<0.0001#	0.81	<0.0001#	0.79	<0.0001#	0.66	<0.0001#	0.48	0.0015	0.40	0.0109
S_{cond} L^{-1}	0.70	<0.0001#	0.68	<0.0001#	0.65	<0.0001#	0.60	<0.0001#	0.28	0.0816	0.41	0.0082
S_{acin} L^{-1}	0.42	0.0068	0.41	0.0095	0.42	0.0072	0.29	0.0722	0.33	0.0349	0.29	0.0739
FEV_1 z-score	−0.66	<0.0001#	−0.68	<0.0001#	−0.62	<0.0001#	−0.56	<0.0001#	−0.39	0.0123	−0.23	0.1452
FVC z-score	−0.56	0.0002#	−0.59	0.0001#	−0.49	0.0014	−0.51	0.0009#	−0.36	0.0213	−0.15	0.3670
RV/TLC %	0.60	<0.0001#	0.62	<0.0001#	0.55	0.0002#	0.50	0.0012#	0.49	0.0012#	0.15	0.3577

Data are presented as Spearman correlation coefficients; for all correlations we performed a Bonferroni correction: 0.05/36, as appropriate. LCI: lung clearance index; S_{cond} and S_{acin}: normalised phase III slope indices (see main text and supplementary material for explanation); FEV_1: forced expiratory volume in 1 s; FVC: functional vital capacity; RV: residual volume; TLC: total lung capacity. Correlation between dedicated morphology MRI score (mean from both readers) and different lung function outcomes: LCI, S_{cond}, S_{acin}, FEV_1, FVC and RV/TLC ratio. Calculation of the correlation between each reader and lung function values determined similar values (data not shown). #: p-values <0.0014 were considered statistically significant.

(supplementary table E4). Calculation of the correlation between the scores of each reader separately and lung function values resulted in similar findings for reader1 and reader2, *e.g.* total morphology score and LCI (r=0.77 for reader1 and r=0.77 for reader2; p<0.0001). Agreement (ICC) between readers was good, with 0.64 for total morphology score and 0.63 for airway wall thickening and bronchiectasis (supplementary table E4).

Discussion

Main findings

Functional MRI reliably detected ventilation and perfusion defects in children at various stages of CF lung disease. The findings differed significantly compared with the group of healthy controls. This is the first study to examine a function–function correlation between two modalities using the combination of a novel proton-based functional MP-MRI technique and N_2-MBW in patients with CF and healthy controls. The extent of ventilation and perfusion impairment detected by functional MRI is physiologically plausible as the correlation with LCI is strong. The main technical advantage of the new MRI technique is the contrast-agent-free application during normal tidal breathing. Structure–function correlation was also strong between an established morphological CF score and LCI [20]. Furthermore, we revealed a good agreement between both readers for morphological MRI scores. The short duration required to obtain functional MRI is especially attractive for application in children, and when considering time constraints in radiology departments and outpatient clinics. This novel MRI technique appears applicable to most lung diseases that are not primarily characterised by interstitial remodelling.

Comparison with previous studies

Technical considerations

Lung imaging for clinical routine or clinical trial outcome assessment should be sensitive, fast, safe, noninvasive and easily applicable even in children, as structural and functional airway pathologies already occur in asymptomatic infants and children with CF [1, 4, 13]. In this study, we performed measurements with a non-contrast-enhanced functional MRI using MP decomposition. This technique has been validated against different modalities, *e.g.* CT, dynamic contrast enhancement MRI and hyperpolarised noble gas MRI, in human and animal models [25, 31–33]. These studies determined a good correlation with dynamic contrast enhancement and hyperpolarised noble gas MRI, and a high test reproducibility. Furthermore, a good reproducibility of the applied functional MRI method in healthy volunteers was shown [34]. Recently, a study using a FD-based self-gated non-contrast-enhanced functional lung imaging technique called SENCEFUL in patients with CF was reported by Veldhoen *et al.* [35]. Results are not directly comparable, as Veldhoen *et al.* [35] also studied adult patients with more severe lung disease and they only assessed impairment of ventilation. Still, they also report a significant difference in ventilation efficiency between patients and controls. Furthermore, despite the slightly more severe course of disease in their population and the different MRI techniques, associations between impairment of ventilation and FEV_1 are surprisingly comparable between studies (r=0.65 and 0.64, respectively). Of note, MP-MRI as used in our study does not measure the information on regional ventilation and perfusion directly, but by the extraction of signal modulations in the lung caused by the change of lung parenchyma density and regional blood flow.

Physiological considerations

Interestingly, we found that lung function changes measured at the mouth based on ventilation distribution efficiency of the whole lung are well associated with impairment in ventilation and perfusion detected by local imaging of the lung. Our data thereby confirm the concept of LCI being a sensitive marker of global ventilation distribution.

To capture the large range of variety in functional disease in CF phenotypes, which may even fluctuate over time, it is of great importance to use multimodal diagnostic technologies [36]. Functional MRI may detect clinically silent pathological processes earlier than even the already very sensitive N_2-MBW. Before morphological changes occur, ventilation/perfusion in the lung is likely to be affected, but may be missed by previous imaging or lung function techniques. The quantification of ventilation/perfusion allows estimating early changes of the latter. This is particularly true with regard to the Euler–Liljestrand reflex, inducing vasoconstriction in unventilated peripheral lung compartments [37]. We chose LCI as the "gold standard" comparator for functional MRI indices because of its high repeatability, specificity and sensitivity to detect global ventilation inhomogeneity, a proxy for both central and peripheral airway involvement in CF [38]. However, global ventilation inhomogeneity is only detected if lung compartments are at least slowly ventilated. S_{cond}, a parameter for convection-dependent ventilation inhomogeneity, strongly correlated with perfusion impairment, bronchiectasis and mucus plugging in the lung, and was moderately correlated with fractional ventilation impairment. A previous study already showed the high

prevalence of elevated S_{cond} values in CF, but did not find a correlation between lung function outcomes. This was explained by the theory that in the presence of a complete obliteration of small airways, S_{cond} will not contribute to convective ventilation [39]. Whether these findings are epiphenomena or a reflection of a true structure–function interaction in small airways needs to be determined in longitudinal studies.

Strengths and limitations

Our findings are strengthened by the rigorously performed study design. We always adhered to the full protocol within a clinical setting and on the same day. The order was thus respected (*i.e.* first functional then morphological sequences). All data were obtained using standard commercially available equipment provided by the manufacturer. Morphological scores are reliable as agreement between both readers was good. However, short- and long-term repeatability require further study. Interestingly, function–function associations using two different but very sensitive techniques seem quite linear over a wide range of disease severity. This cannot be extrapolated to end-stage lung disease and very likely different outcome measures are more suitable in more severe disease.

The functional and morphological MRI protocols required up to 30 min compared with a HRCT scan examination which takes only 5 s. HRCT is currently the "gold standard" for imaging morphological changes of lung disease. Nevertheless, HRCT only provides detailed information on morphological impairment, whereas estimating trapped gas requires repeated scans and breathing manoeuvres. The free tidal breathing in our protocol could have influenced the estimation of the amount of air trapping in the patients [40]. Our study overcomes some risks from previous imaging modalities in CF, *e.g.* allergic sensitisation or anaphylactic reactions to contrast agents, deposition of contrast agents in tissue and cumulative ionising radiation dose, which is especially important as survival is steadily increasing in patients with CF [9, 21, 22].

Clinical relevance

With this study we emphasise the applicability of functional lung MRI in paediatric patients with CF. All MRI measurements were feasible and of good quality. The non-contrast-enhanced protocol, the free tidal breathing during the measurement, the nonionising radiation and the short time to perform functional MRI demonstrate the great advantages compared with commonly used imaging protocols and techniques. The "new era" of less severe disease, heralded by new treatment targets and better therapeutic options, demands sensitive physiological and structural outcomes to prevent irreversible airway changes. Personalised diagnostic tools enable personalised treatment, which currently plays an increasing role in clinical practice. Potentially reversible functional impairment can now be detected before irreversible morphological changes occur in the lungs. We want to draw attention to new functional imaging modalities and their combination with sensitive lung function indices to determine fractional ventilation impairment in the lung. The potential role of this MRI technique for other lung diseases, such as primary ciliary dyskinesia, chronic obstructive pulmonary disease or asthma, has to be investigated in future studies.

Conclusions

Functional MRI of the lung is feasible in children over 5 years of age and a promising diagnostic technique. Fractional ventilation and relative perfusion impairment of the lung correlate strongly with the LCI in patients with CF. Functional MRI has the potential to detect fractional ventilation and relative perfusion inhomogeneities, which may be the earliest changes of the airways and potentially still reversible. While confirmation in larger cohorts seems to be required, our results may promote the application of MRI as a quantitative morphological and functional test in chronic lung diseases such as CF.

Acknowledgements

The authors would like to thank all of the children and their families for their participation in the study. The authors would also like to express their thanks especially to Sharon Schmidt, Linn Krueger, Tobias Ehrenreich, Sophie Yammine, Chiara Abbas (Inselspital, Bern University Hospital, University of Bern, Bern, Switzerland); Bernd Jung, Michael Ith (Dept of Interventional and Pediatric Radiology, Inselspital, Bern University Hospital, Bern, Switzerland); Tanja Haas (Dept of Radiology, Division of Radiological Physics, University of Basel Hospital, Basel, Switzerland); and Philippe C. Cattin, Robin Sandkühler (Dept of Biomedical Engineering, University of Basel, Allschwil, Switzerland); and to all the study nurses and medical-technical assistants from the Dept of Radiology (Inselspital, Bern University Hospital, University of Bern, Bern, Switzerland) for their patient care, support in measurements and recruitment of children.

Author contributions: S. Nyilas, G. Bauman, O. Pusterla, U. Frey, C. Casaulta, O. Bieri and P. Latzin designed the study concept. S. Nyilas collected study data. S. Nyilas, G. Bauman, G. Sommer and E. Stranzinger analysed the data. S. Nyilas, G. Bauman, G. Sommer, E. Stranzinger, O. Pusterla, U. Frey, I. Korten, F. Singer, C. Casaulta, O. Bieri and P. Latzin interpreted the data. S. Nyilas and G. Bauman drafted the manuscript. All authors revised the manuscript.

References

1 Grasemann H, Ratjen F. Early lung disease in cystic fibrosis. *Lancet Respir Med* 2013; 1: 148–157.
2 Davies J, Sheridan H, Bell N, *et al.* Assessment of clinical response to ivacaftor with lung clearance index in cystic fibrosis patients with a G551D-CFTR mutation and preserved spirometry: a randomised controlled trial. *Lancet Respir Med* 2013; 1: 630–638.
3 Ratjen F, Hug C, Marigowda G, *et al.* Efficacy and safety of lumacaftor and ivacaftor in patients aged 6–11 years with cystic fibrosis homozygous for F508del-CFTR: a randomised, placebo-controlled phase 3 trial. *Lancet Respir Med* 2017; 5: 557–567.
4 Tiddens HA. Detecting early structural lung damage in cystic fibrosis. *Pediatr Pulmonol* 2002; 34: 228–231.
5 Ramsey KA, Rosenow T, Turkovic L, *et al.* Lung clearance index and structural lung disease on computed tomography in early cystic fibrosis. *Am J Respir Crit Care Med* 2016; 193: 60–67.
6 Singer F, Kieninger E, Abbas C, *et al.* Practicability of nitrogen multiple-breath washout measurements in a pediatric cystic fibrosis outpatient setting. *Pediatr Pulmonol* 2013; 48: 739–746.
7 Gustafsson PM, Robinson PD, Gilljam M, *et al.* Slow and fast lung compartments in cystic fibrosis measured by nitrogen multiple-breath washout. *J Appl Physiol* 2014; 117: 720–729.
8 Nyilas S, Schlegtendal A, Singer F, *et al.* Alternative inert gas washout outcomes in patients with primary ciliary dyskinesia. *Eur Respir J* 2017; 49: 1600466.
9 Pearce MS, Salotti JA, Little MP, *et al.* Radiation exposure from CT scans in childhood and subsequent risk of leukaemia and brain tumours: a retrospective cohort study. *Lancet* 2012; 380: 499–505.
10 Kuo W, Ciet P, Tiddens HA, *et al.* Monitoring cystic fibrosis lung disease by computed tomography. Radiation risk in perspective. *Am J Respir Crit Care Med* 2014; 189: 1328–1336.
11 O'Connor OJ, Vandeleur M, McGarrigle AM, *et al.* Development of low-dose protocols for thin-section CT assessment of cystic fibrosis in pediatric patients. *Radiology* 2010; 257: 820–829.
12 Walkup LL, Thomen RP, Akinyi TG, *et al.* Feasibility, tolerability and safety of pediatric hyperpolarized ^{129}Xe magnetic resonance imaging in healthy volunteers and children with cystic fibrosis. *Pediatr Radiol* 2016; 46: 1651–1662.
13 Wielpütz MO, Puderbach M, Kopp-Schneider A, *et al.* Magnetic resonance imaging detects changes in structure and perfusion, and response to therapy in early cystic fibrosis lung disease. *Am J Respir Crit Care Med* 2014; 189: 956–965.
14 Fain S, Schiebler ML, McCormack DG, *et al.* Imaging of lung function using hyperpolarized helium-3 magnetic resonance imaging: review of current and emerging translational methods and applications. *J Magn Reson Imaging* 2010; 32: 1398–1408.
15 Mugler JP, Altes TA. Hyperpolarized ^{129}Xe MRI of the human lung. *J Magn Reson Imaging* 2013; 37: 313–331.
16 Smith L, Marshall H, Aldag I, *et al.* Longitudinal assessment of children with mild CF using hyperpolarised gas lung MRI and LCI. *Am J Respir Crit Care Med* 2017; in press [https://doi.org/10.1164/rccm.201705-0894LE].
17 Edelman RR, Hatabu H, Tadamura E, *et al.* Noninvasive assessment of regional ventilation in the human lung using oxygen-enhanced magnetic resonance imaging. *Nat Med* 1996; 2: 1236–1239.
18 Wielpütz MO, Mall MA. MRI accelerating progress in functional assessment of cystic fibrosis lung disease. *J Cyst Fibros* 2017; 16: 165–167.
19 Wielpütz MO, Eichinger M, Biederer J, *et al.* Imaging of cystic fibrosis lung disease and clinical interpretation. *Rofo* 2016; 188: 834–845.
20 Stahl M, Wielputz MO, Graeber SY, *et al.* Comparison of lung clearance index and magnetic resonance imaging for assessment of lung disease in children with cystic fibrosis. *Am J Respir Crit Care Med* 2017; 195: 349–359.
21 Costello JR, Kalb B, Martin DR. Incidence and risk factors for gadolinium-based contrast agent immediate reactions. *Top Magn Reson Imaging* 2016; 25: 257–263.
22 McDonald RJ, McDonald JS, Kallmes DF, *et al.* Intracranial gadolinium deposition after contrast-enhanced MR imaging. *Radiology* 2015; 275: 772–782.
23 Bauman G, Bieri O. Matrix pencil decomposition of time-resolved proton MRI for robust and improved assessment of pulmonary ventilation and perfusion. *Magn Reson Med* 2017; 77: 336–342.
24 Bieri O. Ultra-fast steady state free precession and its application to *in vivo* ^{1}H morphological and functional lung imaging at 1.5 tesla. *Magn Reson Med* 2013; 70: 657–663.
25 Bauman G, Puderbach M, Heimann T, *et al.* Validation of Fourier decomposition MRI with dynamic contrast-enhanced MRI using visual and automated scoring of pulmonary perfusion in young cystic fibrosis patients. *Eur J Radiol* 2013; 82: 2371–2377.
26 Eichinger M, Optazaite DE, Kopp-Schneider A, *et al.* Morphologic and functional scoring of cystic fibrosis lung disease using MRI. *Eur J Radiol* 2012; 81: 1321–1329.
27 Robinson PD, Latzin P, Verbanck S, *et al.* Consensus statement for inert gas washout measurement using multiple- and single-breath tests. *Eur Respir J* 2013; 41: 507–522.
28 Miller MR, Hankinson J, Brusasco V, *et al.* Standardisation of spirometry. *Eur Respir J* 2005; 26: 319–338.
29 Anagnostopoulou P, Jensen R, Kranz N, *et al.* New reference values for N_2 multiple breath washout outcomes in pre-school and school-aged children. *Eur Respir J* 2016; 48: PA371.
30 Portney L, Watkins M. Foundations of Clinical Research: Application to Practice. Stamford, Appleton & Lange, 1993.
31 Bauman G, Lützen U, Ullrich M, *et al.* Pulmonary functional imaging: qualitative comparison of Fourier decomposition MR imaging with SPECT/CT in porcine lung. *Radiology* 2011; 260: 551–559.
32 Bauman G, Puderbach M, Deimling M, *et al.* Non-contrast-enhanced perfusion and ventilation assessment of the human lung by means of Fourier decomposition in proton MRI. *Magn Reson Med* 2009; 62: 656–664.
33 Bauman G, Scholz A, Rivoire J, *et al.* Lung ventilation- and perfusion-weighted Fourier decomposition magnetic resonance imaging: *in vivo* validation with hyperpolarized ^{3}He and dynamic contrast-enhanced MRI. *Magn Reson Med* 2013; 69: 229–237.
34 Lederlin M, Bauman G, Eichinger M, *et al.* Functional MRI using Fourier decomposition of lung signal: reproducibility of ventilation- and perfusion-weighted imaging in healthy volunteers. *Eur J Radiol* 2013; 82: 1015–1022.

35 Veldhoen S, Weng AM, Knapp J, *et al.* Self-gated non-contrast-enhanced functional lung MR imaging for quantitative ventilation assessment in patients with cystic fibrosis. *Radiology* 2017; 283: 242–251.
36 Nyilas S, Singer F, Kumar N, *et al.* Physiological phenotyping of pediatric chronic obstructive airway diseases. *J Appl Physiol* 2016; 121: 324–332.
37 Paddenberg R, Mermer P, Goldenberg A, *et al.* Videomorphometric analysis of hypoxic pulmonary vasoconstriction of intra-pulmonary arteries using murine precision cut lung slices. *J Vis Exp* 2014; (83): e50970.
38 Aurora P, Stanojevic S, Wade A, *et al.* Lung clearance index at 4 years predicts subsequent lung function in children with cystic fibrosis. *Am J Respir Crit Care Med* 2011; 183: 752–758.
39 Horsley AR, Macleod KA, Robson AG, *et al.* Effects of cystic fibrosis lung disease on gas mixing indices derived from alveolar slope analysis. *Respir Physiol Neurobiol* 2008; 162: 197–203.
40 Bonnel AS, Song SMH, Kesavarju K, *et al.* Quantitative air-trapping analysis in children with mild cystic fibrosis lung disease. *Pediatr Pulmonol* 2004; 38: 396–405.